Speed-up Chromatic Sensors by Optimized Optical Filters

Miro Taphanel[a], Bastiaan Hovestreydt[a] and Jürgen Beyerer[b]

[a]Vision and Fusion Laboratory IES, Karlsruhe Institute of Technology KIT, Germany;
[b]Fraunhofer Institute of Optronics, System Technologies and Image Exploitation IOSB, Karlsruhe, Germany

Keywords: interference filter optimization, thin film filter, inline 3D sensor, high-speed measurement

1. INTRODUCTION

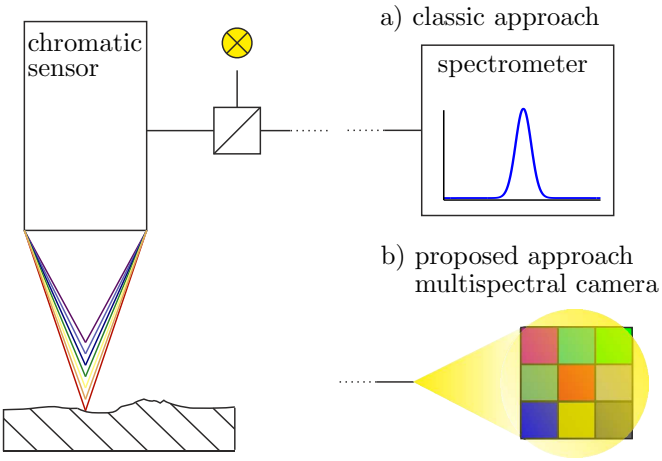

Figure 1. Visualization of the proposed idea: Replacing a spectrometer by a multispectral camera. Take advantage of faster frame rates and keep measurement resolution high by optimized filters.

The probably best known chromatic sensor is the chromatic confocal point sensor,[1] which is an optical displacement sensor (depicted in Fig. 1). It uses different wavelengths to encode the distance and has one measurement spot. Beside this prominent example, there are plenty of other realizations. E.g. Lee[2] lists fiber optical sensors which measure temperature, displacement, current, strain and more. A variant of the chromatic confocal point sensor is used within this paper as example to apply the proposed method, referred to as CCT (*chromatic confocal triangulation*) sensor.[3] In contrast to the point sensor the CCT sensor has many measurement spots next to each other (typically 2000 measurement spots in a row).

The idea of the chromatic principle is to encode measurement information as spectral information. Each distinguishable measurement value corresponds to a unique spectral distribution of the optical signal. Usually, a spectrometer is used to sample this spectrum and the measurement value is determined by additional signal processing. However, spectrometers are comparable slow because each measurement consists of hundreds of pixels to sample the spectrum of the optical signal. The readout time of such a spectrometer becomes critical, if the number of measurement spots increases. In this case the spectrometer (hyperspectral camera) consists of a full frame sensor and its frame rate limits the measurement frequency.

In this paper a multispectral camera is proposed with a low number of optical filters (depicted in Fig.1b). The optical signal is measured through a set of filters, which are optimized in terms of sensitivity and uniqueness. Hence, each distinguishable spectrum corresponds to a unique grey value vector. This approach can be regarded

Further author information: (Send correspondence to Miro Taphanel)
Miro Taphanel: E-mail: miro.taphanel@kit.edu, Telephone: +49 (0) 721 6091-389
Bastiaan Hovestreydt: E-mail: publications@hovestreydt.com, Telephone: +49 (0) 721 9084-852
Jürgen Beyerer: juergen.beyerer@iosb.fraunhofer.de, Telephone: +49 (0) 721 6091-210

as a generalized kind of color vision, because a multispectral camera implicit spans a multidimensional color space and a grey value vector can be interpreted as a multidimensional color coordinate.[4] The advantage of this approach is obvious; using only a small set of optical filters instead of a spectrometer significantly reduces the acquired data, resulting in an increased measurement speed.

In literature,[5,6] the principle idea using a multispectral camera is well known. However, the possibility of customized and optimized optical filters is not used yet. Instead, simple gaussian like filters are proposed.[7] Furthermore, it is commonly argued in HLS or HSV color space,[8,7] what is an arbitrary reduction to three color channels. In[4] it is shown that the HSV or HLS color spaces are distorted, that can lead to misinterpretation if distances between color coordinates are calculated.

2. PROPOSED METHOD

This section proposes a method how to optimize or customize a multispectral camera for chromatic sensors. More specific, the filters of the multispectral camera will be optimized using interference filter technology. The basic idea is to assign each measurement value of interest to an unique n-dimensional color coordinate. The application dependent optics of chromatic sensors already encodes different measurement value of interest by unique spectra. By using a multispectral camera with n filters each spectrum corresponds to a n dimensional color coordinate. The exact coordinates are controlled by the filter transmission characteristics and will be optimized in terms of sensitivity and uniqueness of the overall system.

In the first subsection the relationship between color coordinate and measurement value of interest is derived, namely the forward model. This model consists of a general model of a multispectral camera and the relationship between measurement value of interest and underlying spectrum. Unfortunately, this relationship is application depended. To make this method easily applicable to other chromatic sensors, it is attempted to highlight application dependent issues.

The second subsection tackles the optimization procedure. Two merit functions are proposed, one rating the system sensitivity and another one rating the uniqueness of a measurement. These merit functions are used in a minimax optimization to optimize the interference filters of the multispectral camera. During optimization thin film layer thicknesses of interference filters are adjusted.

2.1 FORWARD MODEL

2.1.1 Modeling a multispectral camera

A multispectral camera with n filters implicitly spans a n-dimensional color* space. Then a grey value vector $\mathbf{g} = (g_1, \ldots, g_n)^\top$ defines a coordinate in this space. For an acquisition of light with spectral distribution $s(\lambda)$ the following relationship can be formulated:[4]

$$\mathbf{g} = a \int_T \int_A \int_\Lambda \int_\Omega q(\lambda)\mathbf{f}(\lambda, \mathbf{p}, \alpha)s(\lambda)\mathrm{d}\Omega\mathrm{d}\lambda\mathrm{d}A\mathrm{d}T. \tag{1}$$

Each scalar $g_i \in \mathbf{g}$ is described as functional using four integrals over time T, pixel area A, wavelength Λ, and solid angle Ω, respectively. The integrand consists of the light spectrum $s(\lambda)$ weighted according the quantum efficiency $q(\lambda)$ and the filter transmission characteristic $\mathbf{f}(\lambda, \mathbf{p}, \alpha) = (f_1, \ldots, f_n)^\top$. The parameter vector $\mathbf{p}$ describes thin film layer thicknesses and indicates that these filters $\mathbf{f}(\lambda, \mathbf{p}, \alpha)$ will be optimized later on. Because interference filters are highly sensitive to the angle of incidence α, it is taken into account, too. The scaling variable a avoids unessential unit calculations and quantization is neglected. This camera model can be simplified using the assumptions of no time dependences of the integrand nor spatial variation within one pixel. Furthermore, the chief ray is assumed to be perpendicular to the interference filters and a symmetric illumination cone with solid angle $\Omega = 2\pi(1 - \cos(\alpha_{\max}))$ is assumed, too. Then $\mathbf{g}$ simplifies to:

$$\mathbf{g} = a \int_\Lambda \left(\int_0^{\alpha_{\max}} \mathbf{f}(\lambda, \mathbf{p}, \alpha) 2\pi \sin(\alpha)\mathrm{d}\alpha \right) q(\lambda)s(\lambda)\mathrm{d}\lambda \; AT. \tag{2}$$

*One could argue that color is directly related to human color perception which is by definition three dimensional. However, in this paper a multispectral camera is considered as a generalized kind of color vision and the three dimensional human color perception is just a special case.

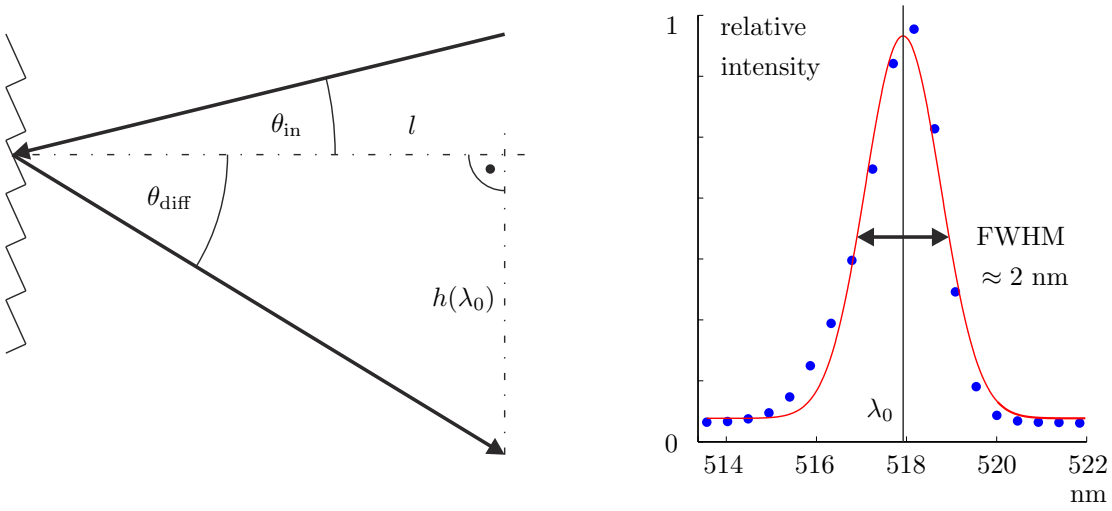

(a) (b)

Figure 2. On the left hand side (a), the grating equation is depicted in a CCT sensor like setup. The chromatic optics of the CCT sensor uses a grating to illuminate different heights with different wavelengths.[3] On the right hand side (b) a measurement of the optical signal is shown. An average of 100 measurements is shown, using a Ocean Optics HR2000+ spectrometer and the CCT prototype presented in.[3] A gaussian model is fitted with central wavelength λ_0.

2.1.2 Modeling the spectral behavior of a chromatic sensor

Based on camera model (2) the forward model is obtained, if the relationship between measurement value of interest h and corresponding spectrum $s(\lambda, h)$ is included. Unfortunately, this relationship is purely application dependent and must be reformulated if another sensor concept is used.

In this paper the CCT sensor is used as example application. It is a chromatic confocal 3D sensor and the measurement value of interest is the surface height h. The chromatic optics causes a nearly monochromatic spectrum with a central wavelength λ_0, that corresponds to the current surface height h_0. The spectrum $s(\lambda, h)$ is modeled gaussian like with a FWHM of 2 nm. The only shape parameter that is assumed to be variable is the central wavelength λ_0. As shown in Fig. 2(b), it is only an approximation. The central wavelength λ_0 and the corresponding height h_0 are linked according to the grating equation,[9] depicted in Fig. 2(a). The grating is used within the CCT concept to illuminate different heights with different wavelengths. Taking the CCT setup into account, the following relationship can be formulated:

$$\sin(\theta_{\text{diff}}) = \sin(\theta_{\text{in}}) + m\frac{\lambda_0}{d}, \text{ with } m = 0, \pm 1, \ldots \tag{3}$$

$$\lambda_0(h_0) = \left[\sin\left(\operatorname{atan}\left(\frac{h_0}{l}\right)\right) - \sin(\theta_{\text{in}})\right]\frac{d}{m} \tag{4}$$

The parameters $\{l, \theta_{\text{in}}, m, d\}$ describe the concrete optical setup depicted in Fig. 2 and are unimportant at the moment.

By including this relationship (4) into the camera model (2) the forward model is obtained. The approximation of a spectrum with constant shape has the advantage, that the forward model can be further simplified using a convolution.

$$\mathbf{g}(h_0) = a\int_{\Lambda}\left(\int_0^{\alpha_{\max}} \mathbf{f}(\lambda, \mathbf{p}, \alpha) 2\pi \sin(\alpha) \mathrm{d}\alpha\right) q(\lambda) s(\lambda - \lambda_0(h_0)) \mathrm{d}\lambda \tag{5}$$

$$= a\left(s(\lambda) * \int_0^{\alpha_{\max}} q(\lambda)\mathbf{f}(\lambda, \mathbf{p}, \alpha) 2\pi \sin(\alpha) \mathrm{d}\alpha\right)(\lambda_0(h_0)) \tag{6}$$

2.1.3 Noisy extension of the forward model

Finally, the model is extended in terms of noise. The main source of noise is assumed to be photon noise covered by the camera noise. The camera noise model is chosen according to[10] with a assumption of normal like distributed grey values $\mathbf{G} \sim \mathcal{N}(\mathbf{g}_0, \Sigma)$:

$$\mathrm{E}\{\mathbf{G}(h_0)\} = \mathbf{g}(h_0) \tag{7}$$

$$\Sigma(\mathbf{g}(h_0)) = \begin{pmatrix} \sigma^2(g_1(h_0)) & \cdots & 0 \\ \vdots & \ddots & \vdots \\ 0 & \cdots & \sigma^2(g_n(h_0)) \end{pmatrix} \tag{8}$$

$$\sigma^2(g_i) = \sigma^2_{\mathrm{dark}} + k g_i(h_0) \tag{9}$$

The diagonal matrix Σ shows, that each color channel is assumed to be uncorrelated. To determine meaningful values for σ_{dark} and k the noise of the target camera was measured. Fig.3(a) shows that this simple camera model fits well and $\sigma^2_{\mathrm{dark}} = 0.1$ and $k = 0.5/255$ are good parameters. However, a lot of noise sources are neglected, like temperature influences, fabrication tolerances, especially the interference filter thin film deposition process, aging effects, vibrations, or stray light, just to mention a few. Because the impact of these sources is unknown, one way to deal with it is to increase the camera noise parameters. Then, the optimized multispectral camera should be capable to tolerate additional external noise influences ($\sigma^2_{\mathrm{dark}} = 1$ and $k = 4/255$ were used during optimization). However, this is a critical aspect of the proposed method and must be investigated carefully. A detailed investigation regarding the thin film manufacturing process will be published.[11]

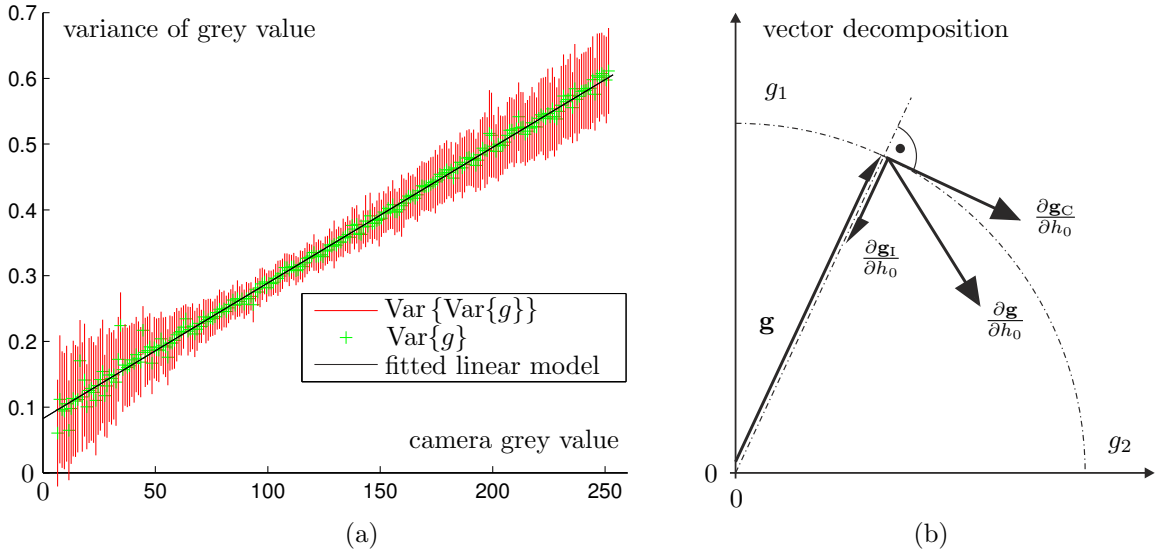

Figure 3. On the left hand side (a), noise measurement of a line scan camera (brand name ELiiXA) with fitted linear model according to Jähne.[10] On the right hand side (b), a two dimensional vector decomposition of a grey value gradient is depicted. A change in $\mathbf{g}$ is split up into a change in intensity $\mathbf{g}_I$ and chromaticity $\mathbf{g}_C$. Further details can be found in.[4]

2.2 Filter Optimization

On basis of the forward model two merit functions are derived, each covered in a single subsection. First of all, a merit function that tries to increase the measurement sensitivity of the sensor. A second one takes care of uniqueness of a measurement to ensure that two measurement values never share the same color coordinate. Both merit functions are used in a minimax optimization. Section 2 concludes with general optimization aspects.

2.2.1 Sensitivity Merit Function

Before it is possible to define a merit function that rates sensitivity, one special aspect of chromatic sensors must be taken into account. The idea of chromatic sensors is to encode measurement values by unique spectra, or more specific by the spectral shape. In consequence, a change of the light intensity, camera integration, or sensor aperture should not affect the measurement result. Due to technical reasons like long term stability, absolut grey values $\mathbf{g}$ are avoided. Instead, intensity normed chromaticity grey values $\mathbf{g}_C$ are preferred. Usually, intensity normed color spaces are used for this purpose. In[4] several commonly used color spaces are compared (e.g. HSV, Lab,...), which distinguish between intensity and chromaticity. However, all these color space transformation are not distance-preserving and usually a multidimensional extension does not exist. Especially the non distance-preserving property prohibits the usage of such a intensity normed color space representation, because the euclidean distance will be used within the merit functions. As alternative, it is proposed to split up the sensitivity term into changes in intensity and chromaticity, but formulated in the unmodified n-dimensional color space of the multispectral camera.

High sensitivity is achieved, if small changes of the measurement value h_0 cause big changes in $\mathbf{g}(h_0)$. Then, with the forward model in mind, a high gradient $\frac{\partial \mathbf{g}}{\partial h_0}$ is preferred. As mentioned above, only changes in chromaticity are relevant. Utilize the fact, that changes in intensity are always† directed towards the origin of a color space, the changes in chromaticity can be obtained by a vectorial decomposition of $\mathbf{g}$(depicted in Fig. 3(b))

$$\frac{\partial \mathbf{g}_C(h_0,\mathbf{p})}{\partial h_0} = \frac{\partial \mathbf{g}(h_0,\mathbf{p})}{\partial h_0} - \frac{\partial \mathbf{g}_I(h_0,\mathbf{p})}{\partial h_0} \tag{10}$$

$$= \frac{\partial \mathbf{g}}{\partial h_0} - \frac{\left(\frac{\partial \mathbf{g}}{\partial h_0}\right)^\top \mathbf{g}}{\mathbf{g}^\top \mathbf{g}}\mathbf{g}, \tag{11}$$

with indices $\mathbf{g}_C$ for chromaticity and $\mathbf{g}_I$ for intensity. The grey value vector $\mathbf{g}$ is calculated according the forward model and $\frac{\partial \mathbf{g}}{\partial h_0}$ is given by:

$$\frac{\partial \mathbf{g}(\lambda(h_0))}{\partial h_0} = \frac{\partial \mathbf{g}(\lambda(h_0))}{\partial \lambda}\frac{\partial \lambda(h_0)}{\partial h_0} \tag{12}$$

$$\frac{\partial \mathbf{g}(\lambda(h_0))}{\partial h_0} = a\left(\frac{\partial s(\lambda)}{\partial \lambda} * \int_0^{\alpha_{\max}} q(\lambda)\mathbf{f}(\lambda,\mathbf{p},\alpha)2\pi\sin(\alpha)\mathrm{d}\alpha\right)(\lambda(h_0)) \cdot \cos\left(\operatorname{atan}\left(\frac{h_0}{l}\right)\right)\frac{1}{1+(\frac{h_0}{l})^2}\frac{d}{ml}. \tag{13}$$

The first term is related to the camera model, the second one is the derivate of equation (4), which is application dependent. Finally, the sensitivity merit function is defined as:

$$\mathrm{MF_S}(h_0,\mathbf{p}) = \left\| \frac{\partial \mathbf{g}_C(h_0,\mathbf{p})}{\partial h_0} \right\|_2^{-1}, \tag{14}$$

which utilizes the euclidean distance to rate the change of multidimensional color coordinate caused by a change in h_0. The inner term is inverted, because it is more meaningful to rate the resolution of the system in units of μm per grey value.

2.2.2 Uniqueness Merit Function

The idea of using a multispectral camera is to assign different measurement values to unique multidimensional color coordinates. In a stochastic consideration this statement must be relaxed and it is only possible to argue in terms of probability of correct assignment. This consideration requires to discretize the continuous measurement

†A linear camera model like (2) is assumed. A detailed discussion can be found in.[4]

range, which is a relatively small claim compared to the quantization process of a camera. Assuming a set of k measurement values $h_{i,i} \in [1,k]$ the probability that everything is assigned correctly is given by:[12]

$$P_{\text{correct}} = \sum_{i=1}^{k} P(\mathbf{g} \in \mathcal{R}_i | h_i) P(h_i), \tag{15}$$

while $\mathcal{R}_i$ describes the region within $\mathbf{g}_i$ is the correct assignment for h_i and $P(h_i)$ is describing the a-priori probability that h_i occurs. Unfortunately, this multicategory case of k measurement values can not be solved in closed form. To avoid heavy numerical calculations an approximation is used instead and two simplifications are necessary. First of all, the multicategory problem of k measurement values is reduced to a combinatorial problem, regarding only two measurement values at the same time. In this case the probability of false assignment $P_{\text{error}}(\mathbf{g}_i, \mathbf{g}_j)$ is calculated only between two measurement values, but all possible pairwise combinations out of the k possible measurement values are evaluated. Because no closed form exists to calculate $P_{\text{error}}(\mathbf{g}_i, \mathbf{g}_j)$ a second simplification is used. The probability $P_{\text{error}}(\mathbf{g}_i, \mathbf{g}_j)$ is approximated using the *Bhattacharyya Bound*:[12]

$$P_{\text{error}}(\mathbf{g}_i, \mathbf{g}_j) = P(\mathbf{g} \in \mathcal{R}_j | h_i) + P(\mathbf{g} \in \mathcal{R}_i | h_j) \tag{16}$$

$$\leq \frac{1}{2} \mathrm{e}^{-t}, \text{ with } t = \frac{1}{8} (\mathbf{g}_j - \mathbf{g}_i)^\top \left(\frac{\Sigma_i + \Sigma_j}{2} \right)^{-1} (\mathbf{g}_j - \mathbf{g}_i) + \frac{1}{2} \log \frac{\det\left(\frac{\Sigma_i + \Sigma_j}{2}\right)}{\sqrt{\det \Sigma_i + \Sigma_j}} \tag{17}$$

The Bhattacharyya Bound is only valid for normal distributions. Fortunately, the camera noise is assumed to be normal like distributed and Fig.3(a) shows, that this requirement is met well.

However, this false assignment probability can not be used directly. Regarding the case of two adjacent measurement values h_i and h_j, then the limit of very close values $\lim_{\triangle h \to 0} P_{\text{error}} = 0.5$ results in the maximum possible false assignment probability, which is equal to guessing. These maximal values would dominate the optimization process and to avoid this behavior a distinction by cases is proposed:

$$P_{\text{error}}(\mathbf{g}_i, \mathbf{g}_j) \leq \begin{cases} \frac{1}{2} e^{-t} \\ 0 \qquad \text{if } |h_j - h_i| <_{\triangle} h_{\text{neighbor}} \end{cases} \tag{18}$$

This formulation is quite heuristical, but from a practical point of view, it seems to perform quite well. Finally, the merit function which rates uniqueness is defined as:

$$\text{MF}_{\text{U}} = \max_{h_i, h_j} \{ P_{\text{error}}(\mathbf{g}_i, \mathbf{g}_j) \}, \quad i,j \in [1,k], \tag{19}$$

by returning always the maximum false assignment probability that occurs within the measurement range.

2.2.3 Optimization

The overall merit function is defined as linear combination of:

$$\text{MF} = a\text{MF}_{\text{S}} + b\text{MF}_{\text{U}}. \tag{20}$$

The weights a and b are chosen in such a way, that the units are μm and %. The target values are at least 1μ vertical resolution and less than 1% false assignment probability. Fig. 4 shows the merit function after optimization as a function of λ_0. It could be seen, that the target values are nearly met (1.14μm and $< 1\%$). Furthermore, due to unknown additional noise sources, much higher noise values are used during optimization. Using the measured noise model instead(cmp. Fig.3) the false assignment probability drops below $4 \cdot 10^{-4}\%$. To calculate a minimum resolution, the measurement system must be limited by something. In this case only 8-bit quantization per color channel was simulated. A shift of 1.14μm causes a change of at least one entry of the greyvalue vector everywhere across the 6 mm measurement range. More interesting than resolution is measurement uncertainty, however, it is more complicated to calculate and additional information about other error influences is necessary.

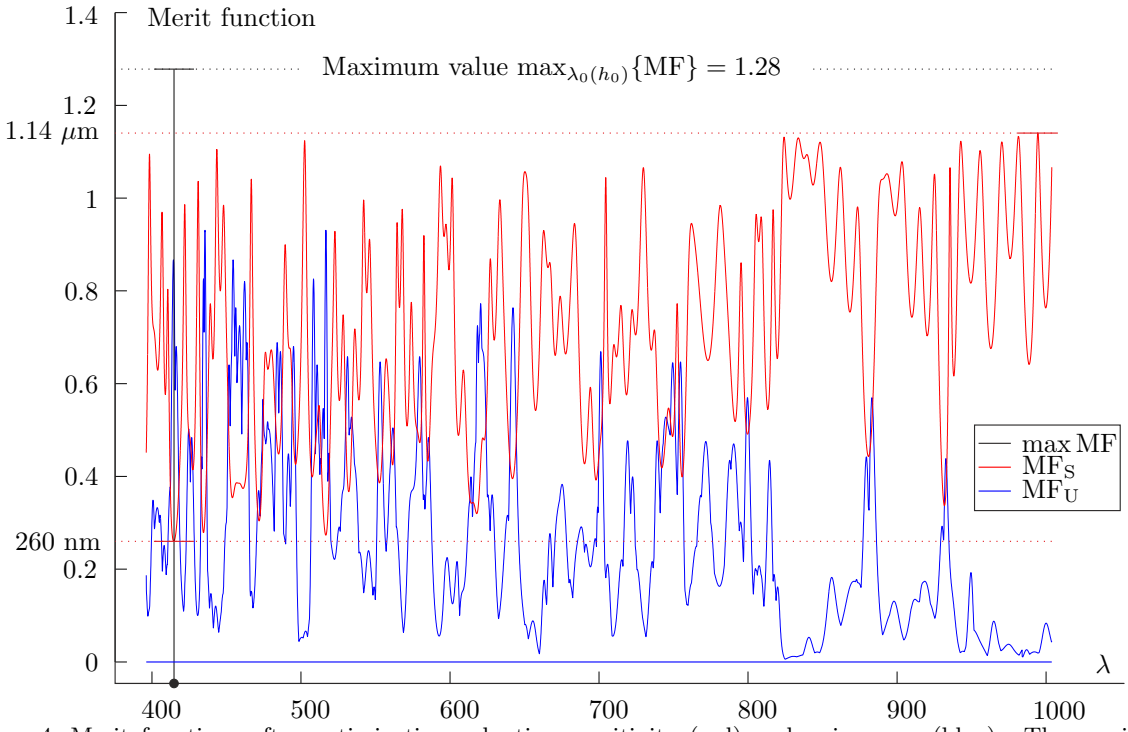

Figure 4. Merit functions after optimization valuating sensitivity (red) and uniqueness (blue). The sensitivity merit function describes the vertical resolution of the CCT sensor in μm, by assuming a 8-bit camera quantization and 6 mm measurement range. The uniqueness merit function is printed twice. Once with high noise values, which were used during optimization and once with the measured noise model. Using the measured noise values results in a straight line near zero ($P_{\mathrm{error}} < 4 \cdot 10^{-4}\%$).

As optimization method a *minimax* algorithm is used.

$$\mathbf{p}^* = \arg\min_{\mathbf{p}\in\mathbb{R}^u} \max_{h_0} \mathrm{MF} \tag{21}$$

In this case, the optimization method notices only the worst working point $\max_{h_0}\{.\}$ within the total measurement range (cmp. Fig. 4 black dashed line). Then, the system overall performance is only as good as its worst working point, which is meaningful for measurement applications. The filter parameter vector $\mathbf{p}^*$ describes the thin film layer thicknesses of the filters and defines a local minimum. The parameter vector is organized as $\mathbf{p} = (\mathbf{p}_1^\top, \ldots, \mathbf{p}_n^\top)^\top$ by arranging all n filter parameter vectors $\mathbf{p}_i, i \in [1, n]$ in a row. This results in a parameter space $\mathbb{R}^u$ with $u = \sum_{i=1}^{n} v; \mathbf{p}_i \in \mathbb{R}^v$. The refractive index of the interference filters are kept fixed during optimization. Due to fabrication aspects, only two coating materials are allowed defining a high and low refractive index. Because all filters are optimized at the same time, the parameter space increases very fast. E.g. 6 Filters, each 41 layers results in a parameter space $\mathbf{p} \in \mathbb{R}^{246}$.

3. RESULTS

As example application a CCT sensor was used to optimize a set of filters for a multispectral camera. A detailed presentation of the sensor can be found in.[3]

The proposed method does not answer the question, how many filters should be used. The minimum possible number of filters is four, because a corresponding intensity normed color space is three dimensional. Three dimensions are necessary to resolve ambiguous color coordinates during optimization (one color coordinate but two corresponding height values). In order to explain this circumstance, some background information is necessary. The function $\mathbf{g}(h_0)$ can be visualized as a path in color space[13],.[3] An ambiguous color coordinate is located at an intersection point of this path. Regarding an intersection point in a two dimensional color space, there is no

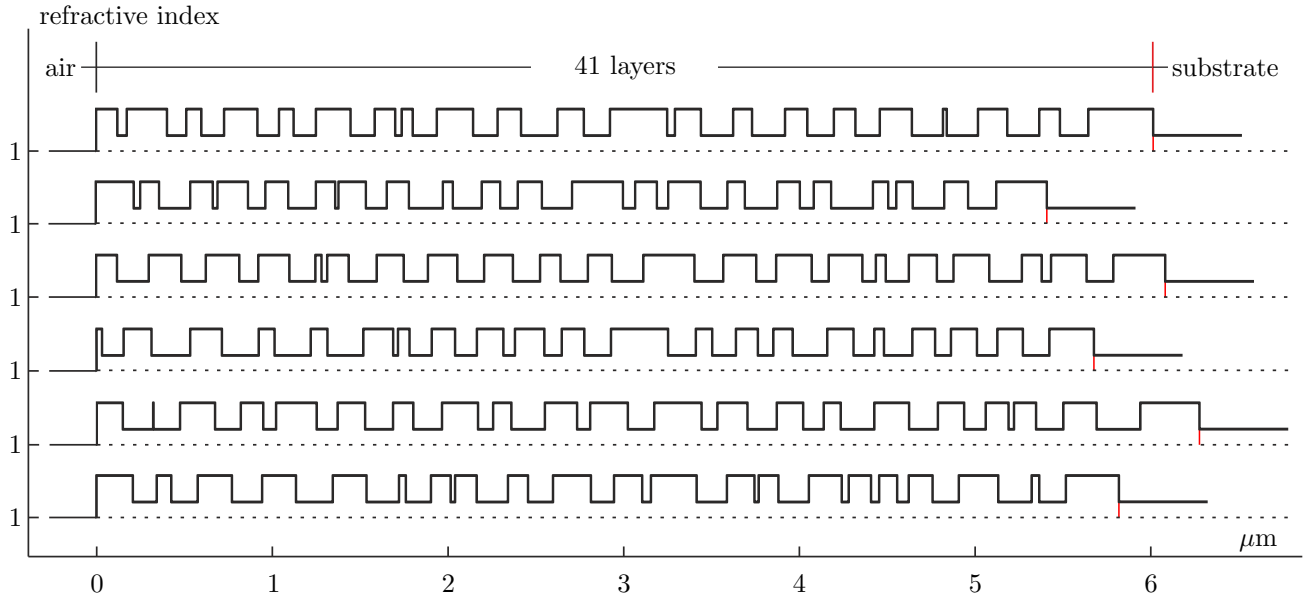

Figure 5. Thin film layer design after optimization. SiO2 (low refractive index $n = 1.46$) and Ta2O5 ($n = 2.29$) were used. Over all thickness about 6 μm and 41 layers per filter.

Table 1. Computational complexity of the optimization process

Integration over angle of incidence using 4th order Gauss-Lobatto	16 sample points
Sample points in wavelength $\triangle\ \lambda = 1$ nm	600 sample points
s- and p-polarization	2 sample points
Numerical gradient based optimization	246 gradients
Number of filter transmission calculations per optimization step	$16 \cdot 2 \cdot 600 \cdot 246 = 4.7 \cdot 10e6$

degree of freedom to resolve this intersection. Adding another filter will increase the dimensionality of the color space and intersection points can be dissolved. On the other side, it is obvious that more filters will simplify the optimization task, especially the influence of noise will decrease in high dimensional spaces and it is getting easier to improve uniqueness during optimization. The authors finally chose six filters, because simulations with more than six filters (e.g. nine) have shown to improve mainly the uniqueness merit function. Another parameter that needs to be defined is the number of thin film layers per interference filter. The authors chose 41 thin film layers per filter and the final layout is depicted in Fig.5.

The starting point for optimization was chosen randomly, but in a way that these randomly created layer thicknesses should be easily manufactured. E.g. keeping a minimum thickness and starting with a thick and high refractive index layer on the glass substrate. As optimization method the minimax algorithm of MATLAB was used. To keep optimization time low, some simplifications were necessary, listed in Table 1. The table also shows, that about five million transmission calculations are necessary per optimization step. The calculations where performed on a Xeon processor (1.9 GHz) and needed less than four days. The interference filter simulation was implemented according Larouche,[14] using the C++ Intel Performance Primitives library. The back reflection of the glass substrate was taken into account, too. Like previously mentioned, a noisier model was used during optimization ($\sigma_{\text{dark}} = 1$ and $\sigma_{\text{max}} = 2.2$ grey values standard deviation). Furthermore, instead of using the measured optical signal with a FWHM = 2 nm, 5 nm was assumed. By taking these higher values the performance will decrease, however the final design is expected to be more tolerant to external uncovered influences.

The simulated filter transmissions after optimization are plotted in Fig.6. The filters look like a signal with higher frequencies at small wavelengths, which is an effect of the physics covered by the interference filter theory. To visualize the effect of high sensitivity dashed lines are inserted. On each dashed line a blue circle marks the position with the highest gradient. It is notable, that at each position only one filter has a high gradient and all

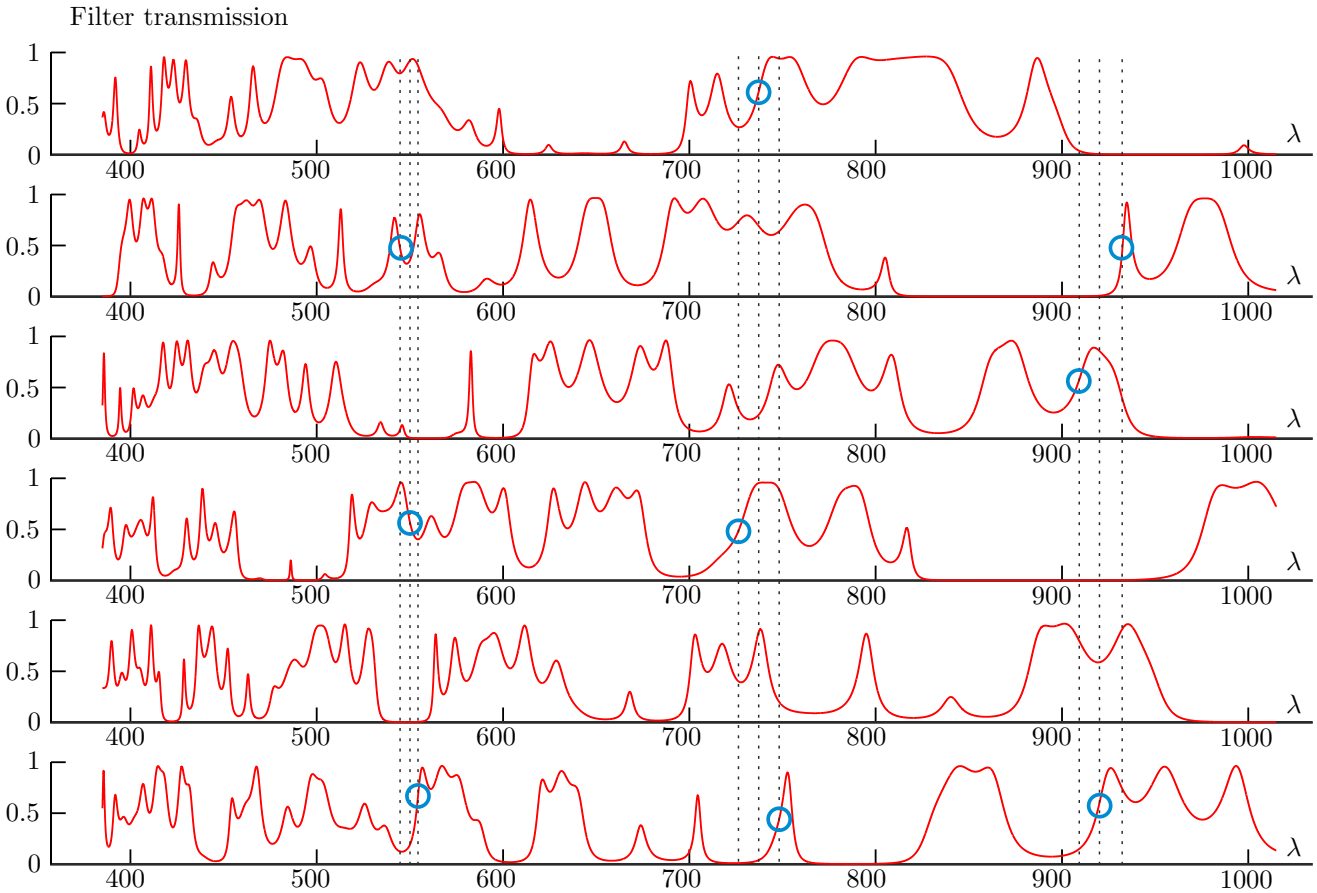

Figure 6. Filter transmission after optimization assuming a cone of illumination of ±6 degree and unpolarized light. Dashed lines allow to compare the filters for a fixed wavelength. Blue circles mark maximum gradients.

others do not. The uniqueness feature can not be seen in these diagrams. However, it seems that the volume of the color space is well used. Every filter consists of longer sections with very low transmission. This is a precondition to also using the border area of the six dimensional color space. As negative example, using six times the same filter would lead to color coordinates located on the diagonal. Finally, the simulated resolution is at least 1.14μm as depicted in Fig.4. To calculate this resolution a limiting factor of 8-bit camera quantization was assumed. In the domain of wavelength, this means that a shift of 0.12 nm of the central wavelength will cause a different color coordinate.

4. CONCLUSIONS AND OUTLOOK TO FUTURE WORK

The proposed method was introduced as a general alternative to spectrometers. It takes advantage of a well defined spectral signal, which is typically for chromatic sensors. In contrast to spectrometers no more additional digital signal processing is necessary. Instead, a multidimensional color coordinate is directly interpreted as a measurement result. The simulated results and the general advantages of this concept, like faster measurement frequencies are promising. The question, if a multispectral camera can have the same performance like a spectrometer needs to be answered by a direct comparison. The development of a prototype is an ongoing project and results will be published.

The main risk of this concept is its inflexibility. The optical filters are optimized under certain assumptions that will never cover all aspects. Uncovered influences can lead the system to fail and a produced set of filters can not be recycled. Using a spectrometer instead, would allow to react with some additional signal processing. For this reason higher noise models and a wider optical signal was used during optimization. Whether this approach increases the tolerance needs to be investigated.

The proposed method itself is partly heuristically motivated (cmp. section 2.2.2). For this reason, it is planed to develop alternative merit functions.

REFERENCES

[1] Leach, R., [*Optical Measurement of Surface Topography*], Springer, 1st edition. ed. (Apr. 2011).

[2] Lee, B., "Review of the present status of optical fiber sensors," *Optical Fiber Technology* **9**, 57–79 (Apr. 2003).

[3] Taphanel, M. and Beyerer, J., "Fast 3D in-line sensor for specular and diffuse surfaces combining the chromatic confocal and triangulation principle," in [*Instrumentation and Measurement Technology Conference (I2MTC), 2012 IEEE International*], 1072 –1077 (May 2012).

[4] Taphanel, M. and Beyerer, J., "Physikalisch motivierte mehrdimensionale farbraumtransformation," in [*Tagungsband Workshop Farbbildverarbeitung*], **18**, 61 –73 (Sept. 2012).

[5] Jones, G. R. and Russell, P. C., "Chromatic modulation based metrology," *Pure and Applied Optics: Journal of the European Optical Society Part A* **2**, 87–110 (Mar. 1993).

[6] Russell, P. C., Spencer, J. W., and Jones, G. R., "Optical fibre sensing for intelligent monitoring using chromatic methodologies," *Sensor Review* **18**, 44–48 (Mar. 1998).

[7] Jones, G. R., Russell, P. C., Vourdas, A., Cosgrave, J., Stergioulas, L., and Haber, R., "The gabor transform basis of chromatic monitoring," *Measurement Science and Technology* **11**, 489–498 (May 2000).

[8] Jones, G. R. G. R., Deakin, A. G., and Spencer, J. W., [*Chromatic Monitoring of Complex Conditions*], CRC Press (2008).

[9] Loewen, [*Diffraction Gratings and Applications*], Taylor & Francis (May 1997).

[10] Jähne, B., [*Digitale Bildverarbeitung*], Springer DE (Mar. 2005).

[11] Taphanel, M., Rademacher, D., and Vergöhl, M., "Impact of thin film fabrication to the optimization process of a multispectral chromatic camera," in [*Optical Interference Coatings*], *OSA Technical Digest*, Optical Society of America (June 2013).

[12] Duda, R. O., Hart, P. E., and Stork, D. G., [*Pattern classification*], Wiley, New York ; Weinheim u.a. (2001).

[13] Taphanel, M., "Filter optimization approach for a chromatic confocal triangulation sensor," in [*Proceedings of the 2012 Joint Workshop of Fraunhofer IOSB and Institute for Anthropomatics, Vision and Fusion Laboratory*], 101 –112, KIT Scientific Publishing, ..., to be published, Karlsruhe (2012).

[14] Larouche, S. and Martinu, L., "OpenFilters: an open source software for the design and optimization of optical coatings," in [*Optical Interference Coatings*], WB6, Optical Society of America (2007).